Dilution and Aspect Ratio Properties on Performance of Laser Deposited Ti-Al-Si-Cu/Ti-6Al-4V Composite Coatings

Dilution and Aspect Ratio Properties on Performance of Laser Deposited Ti-Al-Si-Cu/Ti-6Al-4V Composite Coatings

O.S. Fatoba [1*], LC. Naidoo[2], S.A. Akinlabi[3], E.T. Akinlabi[4], F.M. Mwema[2], O.M. Ikumapayi[2]

[1]College of Aeronautics and Engineering, Kent State University, Ohio, United States of America
[2]Department of Mechanical Engineering, Faculty of Engineering and the Built Environment, University of Johannesburg, South Africa.
[3]Department of Mechanical Engineering, Walter Sisulu University, Butterworth Campus, Eastern Cape, South Africa.
[4]Pan African University for Life and Earth Sciences Institute (PAULESI), Ibadan, Nigeria.
Corresponding author*: drfatobasameni@gmail.com; etakinlabi@gmail.com

Abstract: In spite of the fact that Laser additive manufacturing (AM) processes have a similar material additive manufacturing theory, each AM procedure has its particular features in terms of operational materials and applicable situations. In recent years, additive manufacturing techniques have been acquainted as a promising technique to generate metallic parts since they can annihilate the familiar problems associated with conventional techniques. The results of the investigation showed that as the transverse speed increases, the material that is distributed to the substrate per unit length decreases and therefore that there is an inverse relationship with clad width, melt pool depth and clad height. Hence as the scanning speed increases the width if the height is smaller and the depth of the pool will be smaller too. The results indicate that the specimens manufactured at 900 W, had a decrease in dilution by 3.83%, 1.29% for Ti-Al-11Si-5Cu and Ti-Al-12Si-2Cu respectively when the scanning speed is increased. However, for Ti-Al-13Si-6Cu, there is an increase in the dilution by 1.06%, which can be attributed to the increase of the deposit area below the substrate than above. The results evidently show that increasing the laser scanning speed, increases the aspect ratio of the specimens for laser processing condition 900 W. This relationship is observed in attribution to the clad height being reduced as the scan speed is increased. Moreover, the varying scanning speed influences the clad height more significantly than the clad width; hence, the significant increase in the aspect ratio.

Keywords: Dilution; Aspect Ratio; Volume; Titanium alloy; LMD; Ti-Al-Si-Cu coating

1. Introduction

The Laser Metal Deposition is an additive manufacturing technique which is also known as "Direct Energy Deposition (DED)" and "Laser Cladding (LC)" that employs powder to manufacture complete three-dimensional parts and aids in the repairing of metallic components which are difficult to repair using conventional manufacturing methodologies. The technique also implements a three-dimensional computerised model of the desired product to be manufactured. The DED process is one of the few additive manufacturing processes that utilise powders that provide efficiencies of use which vary from 40-80%. It is courteous to consider environmental and economic factors in relation to the effects that reinforcement powders have on the respective factors. Utilizing a cost-effective powder that may be reused in the process is a method of good environmental and economic consideration [1, 2].

The rate of improvement in the additive manufacturing technologies is immense dating from its earlier introduction in manufacturing decades ago. Its commercial success and great advancements in the different processing techniques used in A.M has drawn in fervent interest from both academia and the world of business [3-5]. The implementation of A.M processes in manufacturing is sustainable since it provides higher efficiencies, accuracy and minimal material waste compared to conventional manufacturing methodologies. A.M technologies have a great potential to bring a radical dynamic shift in the fabrics of society, so much so that its emergence in the manufacturing sector renders conventional manufacturing techniques obsolete [6-8]. AM techniques have leaped over conventional techniques due to the latter failure to produce multifaceted designs, contours and superior microstructures. Researchers around the globe have worked and published several surface modifications techniques but limitations still abound in terms of porosity, high cost, time consuming, and metallurgical bond between the base metal and the reinforcements [9-13].

The properties a titanium material possess is influenced significantly by the morphology of the microstructures. Titanium alloys have their microstructures described by how fine and coarse the texted structures appear and how the lamellar and equiaxed structures are arranged that define the microstructural morphology of the α- and β-phases [14]. The conventional titanium grade alloy that is classified as an (α+β) alloy is Ti-6Al-4V and it is the most commonly used alloy in this category because it offers great versatile balance in properties that interests the aerospace industry to employ it widely in their applications. The essence of this study is to investigate the potentials of modifying the surface integrity and properties of titanium alloy and assess the

outcomes in achieving better structural, mechanical metallurgical properties for varies industrial applications.

2. Methodology

2.1. Materials Specifications and Sample Preparation Method

Titanium alloy grade 5 (Ti-6Al-4V) plates were used as substrates which had a volumetric dimension of 72 x 72 x 5 mm^3. The composition of the titanium substrate in wt.% was 6.12 Al, 0.0039 N, 0.19 Fe, 0.0002 H, 3.76 V, 0.13 O, and Bal. 89.80 Ti. Prior to coating the materials, the substrates were sandblasted to remove the traces of dirt and other impurities. The residue of sand on the materials were washed with water, cleaned with acetone and air dried to facilitate in more absorption and less reflection of the laser beam which is irradiated onto the surface. The coatings were prepared at the National Laser Centre - Council of Scientific and Industrial Research (NLC-CSIR). The Laser Metal Deposition process is conducted using a 3kW (CW) Ytterbium Laser System (YLS-2000-TR) machine which delivered the reinforcement powder into the created molten pool through a concentric nozzle, shielded and carried by Argon gas. The Kuka robot is used in operation with the laser. The particle sizes of the spherical reinforcement powders ranged between 50-150µm. The reinforcement powder used to create the coats composed of a ratio distribution of Ti-Al-Si-Cu as follows: Ti-Al-11Si-5Cu-1.0, Ti-Al-11Si-5Cu-1.2; Ti-Al-12Si-2Cu-1.0; Ti-Al-12Si-2Cu-1.2; Ti-Al-13Si-6Cu-1.0; Ti-Al-13Si-6Cu-1.2 fractions correspondingly. The in-depth mixing of the reinforcements was achieved in 16 hrs at a constant spinning velocity of 72 rpm in a Tube-shaped shaker mixer (T2F).

2 mm separate the three co-axial nozzles and the titanium base metal. The conveying of the mixed homogeneous reinforcements was done via powder feeders at 2.0 g/min. The delivery was done with the protection assistance of the argon inert gas which was put at 2.5 L/min as shown in Figure 1. The intersection of the multiple tracks was achieved at 70% overlap with a track length of 65 mm. The optimal process parameters for the experiment was attained via the design of experiment (DOE). The samples fabrication was done with the optimal process parameters at 1.0-1.2 m/min scan velocity and 900-1000 W laser intensity. The mounted samples followed a grinding and polishing process by using the Struers Polishing Machine, which aided in the removal of resin that covered the surface of interest. The processes rendered the surface reflective and plane in order to carry out the desired material characterization tests. The process was conducted based on the ASTM E3 - 11 standard. The cross-sectional microstructure of the LMD samples was observed by employing an optical microscope and scanning electron microscope. The purpose is to view the microstructure composition and morphology of the

material after laser coating. The analyses of the samples were done by employing the TESCAN machine with an X-MAX instrument to perform scanning electron microscopy (SEM) with electron dispersive spectroscopy (EDS) of the samples. EDS is to ascertain the elemental weights composed within the deposited clad. The analysis is conducted based on ASTM E766-14e1, E986-04 and E1508-12a standards. The BX51M Olympus microscope is used to observe and intuitively study the resulting microstructural features (phase and morphology) of each LMD sample and an unprocessed substrate for baseline data. The microstructural examination is conducted under low and high magnification. The optical microscopy is based on the ASTM E2228-10 standard.

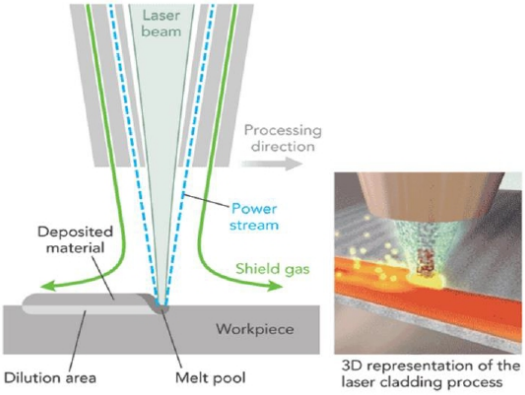

Figure 1: Laser Metal Deposition Machine [15]

3. Result and discussions

Figure 2 presents the SEM image of the Ti-6Al-4V Alloy used in this investigation as the parent material/substrate. The microstructure is at 10X magnification (10 μm). The morphology evidently shows that the structure has equally distributed white and dark phase states which are identified as alpha (α) and beta (β) grains.

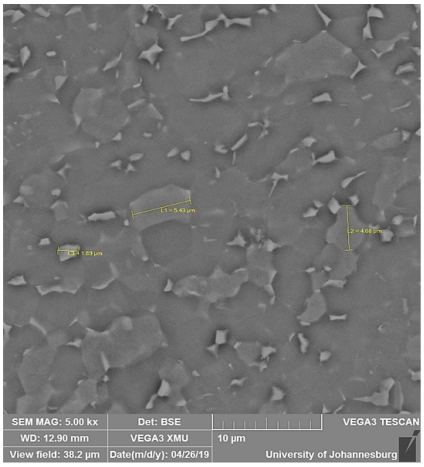

Figure 2: SEM Image of Ti-6Al-4V Alloy

The grains appear to be refined in the direction of the hot-rolled process which was used to fabricate the parent material. The rolling process introduced hot deformation which led to the refining of the grains as well as the direction. There is an aggregate of these grains, appearing polycrystalline in nature. Figure 3 presents the EDS of the parent material (Ti-6Al4V alloy) that is used in the investigation. The magnification is at 5000X. The average grain size of the prominent measured grains is measured to be 3.8 µm. The EDS graph presented as Figure 3 was conducted on the Ti-6Al-4V alloy to ascertain all the elements which is composed in the parent material. It clearly shows that the parent material is enriched with high contents of titanium in addition to aluminium and vanadium as also shown in Table 1.

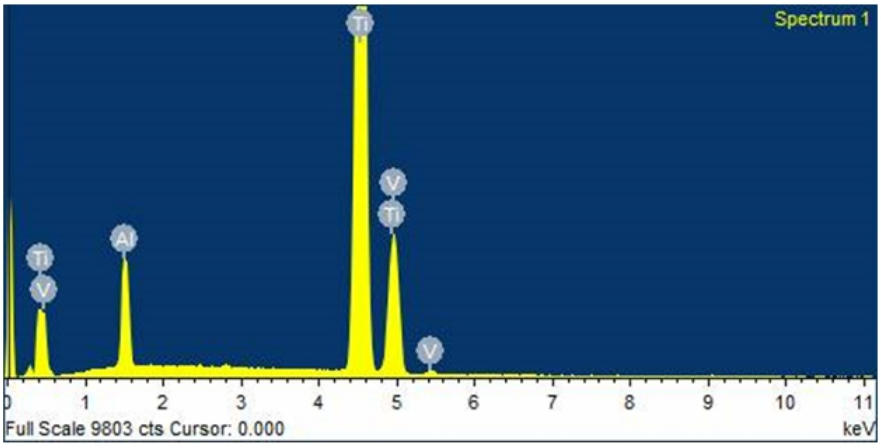

Figure 3: EDS Graph of Ti-6Al-4V Alloy

Table 1: EDS Showing Elemental Composition of Ti-6Al-4V alloy

Element	Weight (%)	Atomic (%)
Titanium (Ti)	90.28	86.52
Aluminium (Al)	5.91	86.52
Vanadium (V)	3.81	3.43
Totals	100	-

The Ti-6Al-4V alloy parent material shown in Table 1 is composed of rich elemental contents of Ti, Al and V. These elements are expected to be traced either independently or formed into intermetallic polycrystal phases in XRD phase identification.

The Laser Energy Density (LED) and Laser Material Interaction Time (LMIT) were computed for the DLMD process as shown in Table 2. The LED is computed to determine the magnitude of processing energy (J/mm^2) that is available to produce the maximum quantity of coating onto the substrate during the process, which is dependent on the direct relation to the laser power and inversely related to the laser scanning speed and the laser beam size. The LMIT is the time measured of the total track length over the laser scanning speed. The LED is computed using the following equation [16]:

$$\mathrm{LED} = \frac{\mathrm{P}}{\mathrm{v_s D_B}} \quad (1)$$

P = Laser Intensity (kW)

v_s = Laser Scanning Speed (m/min)

D_B = Laser Beam Diameter = 2 mm

The LMIT is computed using following equation [17]:

$$\mathrm{LMIT} = \frac{\text{Total Track Length (m)}}{\text{Laser Scanning Speed (m/s)}} \quad (2)$$

Table 2: LED and LMIT Computations

Powder Composition	Sample ID.	Laser Power (W)	Scanning Speed (m/min)	LED (J/mm^2)	LMIT (s)
Ti-Al-11Si-5Cu	1A	900	1	27	3.9
	1B		1.2	22.5	3.25
Ti-Al-12Si-2Cu	4A	900	1	27	3.9

	4B		1.2	22.5	3.25
Ti-Al-13Si-6Cu	5A	900	1	27	3.9
	5B		1.2	22.5	3.25

3.1. Dilution of Deposited Coatings

The dilution shown in Figure 4 quantifies the molten pool mixture of the melted substrate with the reinforcement powders added. This is measured by taking the ratio of the penetration depth of the clad to the combined penetration depth and clad height, as follows [18]:

$$Dilution = \frac{D}{D + H} \quad (3)$$

Where:
D = Penetration depth of deposit (m)
H = Deposit Height (m)

3.2. Aspect Ratio of Deposited Coatings

The aspect ratio shown in Figure 5 is computed by taking the ratio of the deposit width to the deposit height and is expressed as follows [19]:

$$Aspect\ Ratio = \frac{W}{H} \quad (4)$$

Where:
W = Deposit width (m)
H = Deposit height (m)

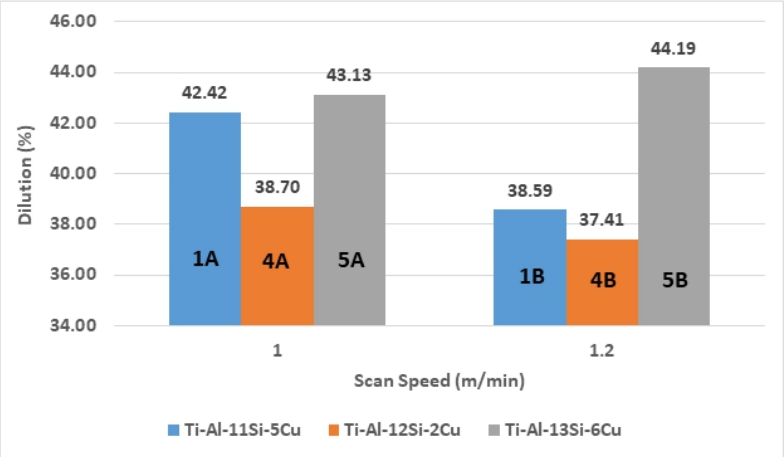

Figure 4: Dilution at 900 W

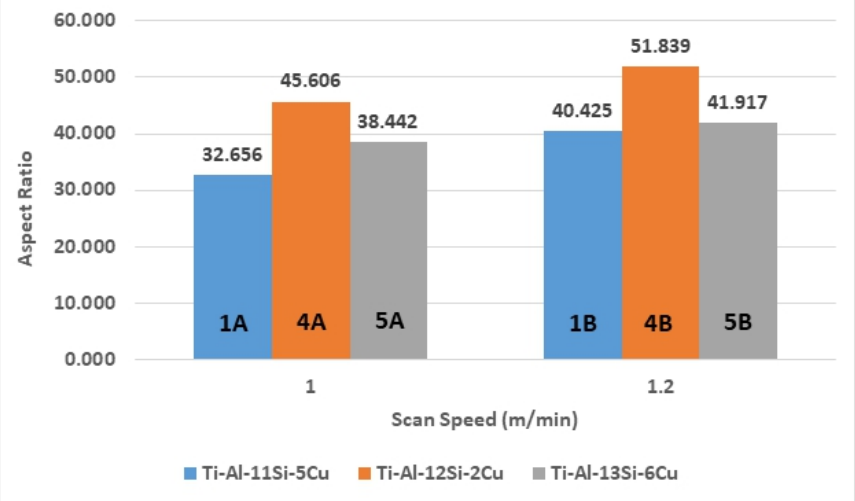

Figure 5: Aspect Ratio at 900 W

Figure 4 provides the graphical results of the relationship of the dilution computed for all the specimens, manufactured at 900 W at a velocity of 1.0.amd 1.2 m/mm respectively, as the scanning speed is increased. Figure 5 shows the results of the aspect ratio computed for the specimens at 900 W at increasing scan speeds. These two geometrical characteristics of the

deposit varied in relation to the increasing scanning speed. The results indicate that the specimens manufactured at 900 W, had a decrease in dilution by 3.83%, 1.29% for Ti-Al-11Si-5Cu and Ti-Al-12Si-2Cu respectively when the scanning speed is increased. However, for Ti-Al-13Si-6Cu, there is an increase in the dilution by 1.06%, which can be attributed to the increase of the deposit area below the substrate than above, which was also found by Gharehbaghi et al. [20]. It is deducible that samples that show a decrease in dilution, have a deposit area ratio in which the above deposit area increased more in relation to the increase of the deposit area below, and vice versa for the specimens that had increased in dilution.

The results evidently show that increasing the laser scanning speed, increases the aspect ratio of the specimens for laser processing conditions at 900 W. This relationship is observed in attribution to the clad height being reduced as the scan speed is increased. Moreover, the varying scanning speed influences the clad height more significantly than the clad width; hence, the significant increase in the aspect ratio [20]. The aspect ratio computations at 900 W reveal the following: The Ti-Al-11Si-5Cu, Ti-Al-12Si-2Cu and Ti-Al-13Si-6Cu samples had increased aspect ratio by 19.22%, 12.02 and 8.29% respectively. Since the samples are overlapped in tracks and all the aspect ratios are greater than five, literature proposes that when it is as such, there should be no inter-run porosity between the overlapped tracks [19]. The aspect ratio is relatively less at 900 W [20].

3.3. Volume and Area of Deposited Coatings

The cross-sectional area for each sample deposit and the volume, are computed according to the work conducted also by Erinosho, et al [21]. The computations show that there is a linear relationship between the area and volume since the volume is dependent on the track length. As previously stated in the methodology, the track length for all the manufactured specimens are constant at 65 mm per tack. The computations of the area and volume are conducted according to the following formulae expressions in equations 5 and 6, and the values are shown in Figure 6:

$$Area = R^2 \cos^{-1}\left(\frac{R-H}{R}\right) - (R-H)\sqrt{2RH - H^2} \quad (5)$$

$$Volume = L[R^2 \cos^{-1}\left(\frac{R-H}{R}\right) - (R-H)\sqrt{2RH - H^2}\,] \quad (6)$$

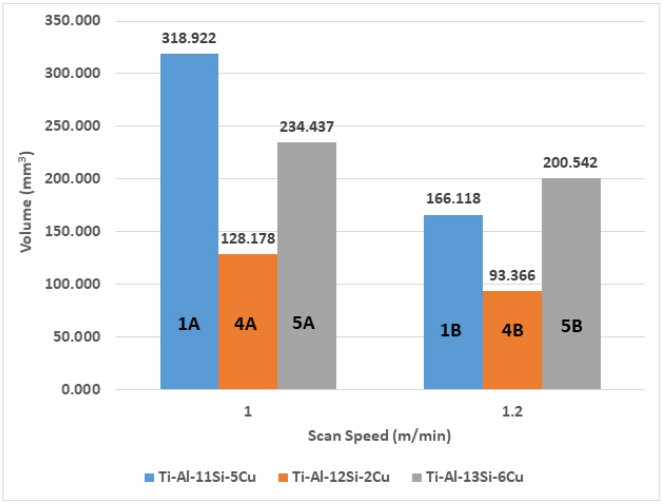

Figure 6: Volume of Deposits at 900 W

Figure 6 graphically represents the relationship of the volume influenced by the varying scan speed at 900 W. The results indicate that there is an inversely proportional relationship between the scanning speed and the volume of the overall deposit, i.e. the volume of the deposit is reduced when the scanning speed is increased. At 900 W, Ti-Al-11Si-5Cu, Ti-Al-12Si-2Cu and Ti-Al-13Si-6Cu reduce in volume by 152.80 mm^3, 34.812 mm^3 and 33.90 mm^3 respectively. Erinosho, et al. [22] also proposed that low scanning speeds create more melt pool which is in attribution of the larger area and volume of cladding. This clearly indicates that at higher laser intensity, there is an increase in the area and volume of the molten pool and solidified clad because the laser and material interaction time is longer which melts more powder in the process. This correlates with the findings of Mary-Jane et al. [23].

3.4. Microstructural Analyses

It is also seen in the SEM images for the best samples, that the microstructure is well-defined and coarsened which consists of the prominent transformed lamellae α+β structures with much noticeable globular alpha phases from prior-β grain boundaries. During the DLMD process, the thermal histories induced in the process led to the promotion of the transformed α+β microstructure from the initial primary α microstructure; the growth and evolution of the distinct grain morphologies and stability of the alpha and beta structures upon increased and reduced structures. These multi-scale microstructures show that coarsened α and α$^{'}$ phases are prominent and formed as acicular structures intermittently, and discretely epitaxial close to the major zones

such as the top of the clad and the fusion zone. Most of the globular grains appear to be promoted at the centre of the clads than above - near the surface of the clad, or below - close to the fusion line. The formation of the large microstructures is attributed to rapid solidification rate [24-27]. Furthermore, the martensitic structures appear near the top of the clad and fusion zone because of rapid solidification in these areas.

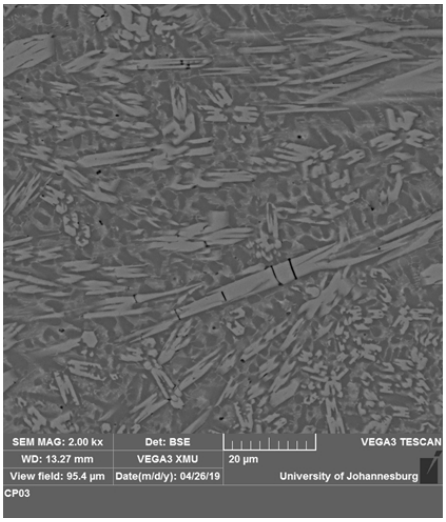

Figure 7: SEM Image of Ti-Al-12Si-2Cu at 900 W and 1.2 m/min

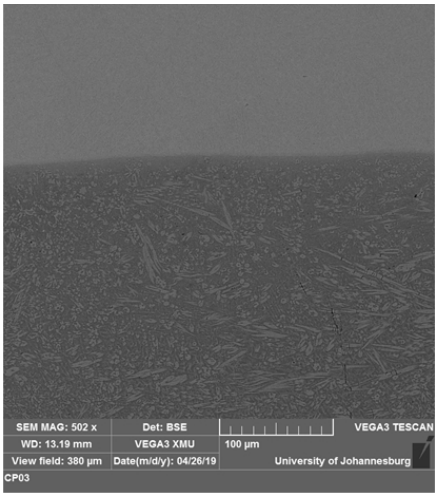

Figure 8: Cross-Section View of Ti-Al-11Si-5Cu at 900 W and 1.2 m/min.

4. Conclusion

- It can be deduced that employing the DLMD additive manufacturing surface engineering technique in improving the surface integrity of Ti-6Al-4V is a successful method when compared to the conventional manufacturing methods used. The results indicate that employing this technique in fabricating Ti-Al-Si-Cu/Ti6Al4V composite can produce quality coatings, given that the processing parameters are optimised.
- Increasing the scanning speed influenced the structural properties as such: the deposit width, height, depth and HAZ, decreased; the aspect ratio increased. The volume of the solidified molten pool had decreased.
- The correct amount of Si and Cu wt.% in the reinforcement powder, in combination with optimized laser intensity and scanning speed, produces composite coating in which the geometrical properties are improved.

Acknowledgements
The authors wish to acknowledge the National Laser Center, CSIR South Africa for the laser equipment.

References

[1] Fatoba, O.S., Akinlabi, E.T. & Akinlabi, S.A. (2018). Numerical Investigation of Laser Deposited Al-Based Coatings on Ti-6Al-4V Alloy. 2018 IEEE 9th International Conference on Mechanical and Intelligent Manufacturing Technologies (ICMIMT 2018), Cape Town, South Africa, pp. 85-90. doi: 10.1109/ICMIMT.2018.8340426.
[2] Fatoba O.S., Akinlabi S.A., Gharehbaghi R. & Akinlabi E.T (2018). Microstructural Analysis, Microhardness and Wear Resistance Properties of Quasicrystalline Al-Cu-Fe Coatings on Ti-6Al-4V Alloy. Materials Express Research. 5(6), 1-14. https://doi.org/10.1088/2053-1591/aaca70.
[3] Cheng, Y. L., Wu, X. Q., Xue, Z. G., Matykina, E., Skeldon, P., & Thompson, G. E. (2013). Microstructure, corrosion and wear performance of plasma electrolytic oxidation coatings

formed on Ti–6Al–4V alloy in silicate-hexametaphosphate electrolyte. Surface and Coatings Technology, 217, 129-139.
[4] Petrovic, V., Vicente Haro Gonzalez, J., Jordá Ferrando, O., Delgado Gordillo, J., Ramón Blasco Puchades, J., & Portolés Griñan, L. (2011). Additive layered manufacturing: sectors of industrial application shown through case studies. International Journal of Production Research, 49(4), 1061-1079.
[5] Chiu, W. K., & Yu, K. M. (2008). Direct digital manufacturing of three-dimensional functionally graded material objects. Computer-Aided Design, 40(12), 1080-1093.
[6] Lipson, H. & Kurman, M. (2010). The Emerging Economy Of Personal Manufacturing Overview and Recommendations. US Office Of Science And Technology Policy, 2010.
[7] Huang, S. H., Liu, P., Mokasdar, A., & Hou, L. (2013). Additive manufacturing and its societal impact: a literature review. The International Journal of Advanced Manufacturing Technology, 67(5-8), 1191-1203.
[8] R. A. of Engineering and Engineering Royal Academy, "Additive Manufacturing: Opportunities And Constraints," *Royal Academy Of Engineering,* no. May 2013, p. 21, 2013.
[9] Adesina, O.S., Popoola, A.P.I. & Fatoba, O.S. (2016). Laser Surface Modification-A focus on the Wear Degradation of Titanium Alloy, Fiber Laser, Dr. Mukul Paul (Ed.), InTech, DOI: 10.5772/61737. Available from: http://www.intechopen.com/books/fiber-laser/
[10] Fatoba, O.S., Adesina, O.S. & Popoola, A.P.I. (2018). Evaluation of microstructure, microhardness, and electrochemical properties of laser-deposited Ti-Co coatings on Ti-6Al-4V Alloy. The International Journal of Advanced Manufacturing Technology. 97(5), 2341-2350. http://dx.doi.org/10.1007/s00170-018-2106-7.
[11] Gharehbaghi, R., Fatoba, O.S. & Akinlabi, E.T. (2018). Experimental Investigation of Laser Metal Deposited Icosahedral Al-Cu-Fe Coatings on Grade Five Titanium Alloy. 2018 IEEE 9th International Conference on Mechanical and Intelligent Manufacturing Technologies (ICMIMT 2018), Cape Town, South Africa, pp. 31-36. doi: 10.1109/ICMIMT.2018.8340416.
[12] Fu, Y., Zhang, X.C., Sui, J.F., Tu, S.T., Xuan, F.Z. & Wang, Z.D. (2015). Microstructure and wear resistance of one-step in-situ synthesized TiN/Al composite coatings on Ti6Al4V alloy by a laser nitriding process. Optics & Laser Technology, 67(0), 4//:78-85.
[13] Weng, F., Chen, C. & Yu, H. (2014a). Research status of laser cladding on titanium and its alloys: a review. Materials & Design, 58:412-425.
[14] Leyens C. & Peters M. (2003). Titanium And Titanium Alloys, Fundamentals And Applications., WILEY-VCH Verlag GmbH & Co. KGaA, Weinheim, ISBN: 3-527-30534-3.
[15] Azam, F. I., Rani, A. M. A., Altaf, K., Rao, T. V. V. L. N., & Zaharin, H. A. (2018). An in-depth review on direct additive manufacturing of metals. In IOP Conf. Ser. Mater. Sci. Eng. 328, 012005.
[16] Schneider, M. F. (1998). Laser cladding. Dimensions. 14, 10.
[17] Mahamood, R. M., Shukla, M., & Pityana, S. (2014). Laser Additive Manufacturing in Surface Modification of Metals. In Surface Engineering Techniques and Applications: Research Advancements (pp. 222-248). IGI Global.
[18] Bruck, G. J. (1988). Fundamentals and industrial applications of high power laser beam

cladding. In Laser Beam Surface Treating and Coating (Vol. 957, pp. 14-28). International Society for Optics and Photonics.

[19] Von Wielligh, L. G. (2008). Characterizing the influence of process variables in laser cladding Al-20WT% Si onto an Aluminium Substrate (Doctoral dissertation). Mandela Metropolitan University, Port Elizabeth, 2008.

[20] Gharehbaghi, R., Fatoba, O.S. & Akinlabi, E.T. (2018). Influence of Scanning Speed on the Microstructure of Deposited Al-Cu-Fe Coatings on a Titanium Alloy Substrate by Laser Metal Deposition Process. 2018 IEEE 9th International Conference on Mechanical and Intelligent Manufacturing Technologies (ICMIMT 2018), Cape Town, South Africa, pp. 44-49. doi: 10.1109/ICMIMT.2018.8340418.

[21] Erinosho, M. F., Akinlabi, E. T., & Pityana, S. (2014). Laser metal deposition of Ti6Al4V/Cu composite: a study of the effect of laser power on the evolving properties. In Proceedings of the World Congress on Engineering (Vol. 2, pp. 1205-206). Newswood Limited Hong Kong.

[22] Erinosho, M. F., Akinlabi, E. T., Johnson, O., & Owolabi, G. (2017). Effect of scannig speed on the material characterisations of laser deposited titanium alloy and copper. University of Johannesburg, Johannesburg.

[23] Obiegbu, M.C. Fatoba, O.S. Akinlabi, E.T. & Akinlabi, S.A (2019). Experimental Study on Characteristics of Laser Metal Deposited Al-Si-Sn-Cu/Ti-6Al-4V composite coatings. Materials Express Research. 6(4), 1-11. https://doi.org/10.1088/2053-1591/aafe4d.

[24] Fatoba O.S; Akinlabi, E.T. & Makhatha, M.E. (2018). Effects of Cooling Rate and Silicon Content on Microstructure and Mechanical Properties of Laser Deposited Ti-6Al-4V Alloy. Materials Today: Proceedings. 5 (9-3), 18368-18375. https://doi.org/10.1016/j.matpr.2018.06.176.

[25] Lan, X., Wu, H., Liu, Y., Zhang, W., Li, R., Chen, S., Zai, X. and Hu, T. (2016). Microstructures and tribological properties of laser cladded Ti-based metallic glass composite coatings. Materials Characterization, 120, 82-89.

[26] Makhatha, M.E., Fatoba, O.S. & Akinlabi, E.T. (2018). Effects of rapid solidification on the microstructure and surface analyses of laser-deposited Al-Sn coatings on AISI 1015 steel. Int J Adv Manuf Technol. 94 (1-4), 773-787. https://doi.org/10.1007/s00170-017-0876-y.

[27] Fatoba O.S., Akinlabi, S.A., Akinlabi E.T. & Krishna S. (2019). Influence of Rapid Solidification and Optimized Laser Parameters Relationship on the Geometrical and Hardness Properties of Ti-Al-Cu Coatings. Materials Today: Proceedings, vol. 18, part 7, 2859-2867. https://doi.org/10.1016/j.matpr.2019.07.153.